

Holistic Approach to Modeling Non-Linear Internal Waves with a Three-Dimensional Nonhydrostatic Model

Principal Investigator: Alberto D. Scotti
Institution: Dept. of Marine Sciences, CB 3300
University of North Carolina, Chapel Hill
UNC, Chapel Hill, NC 27599-3300
Phone: 919-962-9454, Fax: 919-962-1254, Email: ascotti@unc.edu

Co-Principal Investigators: Michael Minion, Sorin Mitran
Institution: Dept. of Mathematics. CB 3250
UNC, Chapel Hill, NC 27599-3250
Phone: 919-962-8475, Fax: 919-962-2586, Email: minion@amath.unc.edu
Phone: 919-843-8901, Fax: 919-962-2586, Email: mitran@amath.unc.edu

Award Number: N00014-05-1-0361
Reporting Period: October 1st, 2006 to September 30, 2007
Report Date: 09/30/2007
Award Period: June 1, 2005 to September 30, 2009

LONG-TERM GOALS

The long-term goal of this project is to develop a numerical model for the simulation of regional processes characterized by a disparity of temporal and spatial scales, such as nonlinear internal waves.

OBJECTIVES

To develop a computational model of large amplitude internal gravity waves that uses adaptive mesh refinement in combination with a numerical scheme of order four or higher, exhibiting minimal numerical dissipation and dispersion. Furthermore, to have the capability of treating realistic topography, thus requiring the capability to describe complicated geometry and also parallel execution to reduce the large computational times intrinsic to three-dimensional simulations.

APPROACH

Physical model

We write the equations of motion as

$$\begin{aligned}\nabla \cdot \vec{u} &= 0 \\ \rho_t + (\vec{u} \cdot \nabla) \rho - N^2 (1 + \beta \rho) v &= 0 \\ (1 + \beta \rho) [\vec{u}_t + (\vec{u} \cdot \nabla) \vec{u}] &= -\nabla p - (\rho - \beta N^2 p) \vec{j} + \frac{v}{\rho} \nabla^2 \vec{u} + \vec{F}\end{aligned}$$

Here all quantities are assumed to be nondimensionalized with reference to a wave length scale L , a time scale $1/N_0$ where N_0 is an average Brunt-Väisälä frequency and ρ_0 an average background

Report Documentation Page				Form Approved OMB No. 0704-0188	
Public reporting burden for the collection of information is estimated to average 1 hour per response, including the time for reviewing instructions, searching existing data sources, gathering and maintaining the data needed, and completing and reviewing the collection of information. Send comments regarding this burden estimate or any other aspect of this collection of information, including suggestions for reducing this burden, to Washington Headquarters Services, Directorate for Information Operations and Reports, 1215 Jefferson Davis Highway, Suite 1204, Arlington VA 22202-4302. Respondents should be aware that notwithstanding any other provision of law, no person shall be subject to a penalty for failing to comply with a collection of information if it does not display a currently valid OMB control number.					
1. REPORT DATE 30 SEP 2007		2. REPORT TYPE Annual		3. DATES COVERED 00-00-2007 to 00-00-2007	
4. TITLE AND SUBTITLE Holistic Approach To Modeling Non-Linear Internal Waves With A Three- Dimensional Nonhydrostatic Model				5a. CONTRACT NUMBER	
				5b. GRANT NUMBER	
				5c. PROGRAM ELEMENT NUMBER	
6. AUTHOR(S)				5d. PROJECT NUMBER	
				5e. TASK NUMBER	
				5f. WORK UNIT NUMBER	
7. PERFORMING ORGANIZATION NAME(S) AND ADDRESS(ES) University of North Carolina, Chapel Hill,Chapel Hill,NC,27599				8. PERFORMING ORGANIZATION REPORT NUMBER	
9. SPONSORING/MONITORING AGENCY NAME(S) AND ADDRESS(ES)				10. SPONSOR/MONITOR'S ACRONYM(S)	
				11. SPONSOR/MONITOR'S REPORT NUMBER(S)	
12. DISTRIBUTION/AVAILABILITY STATEMENT Approved for public release; distribution unlimited					
13. SUPPLEMENTARY NOTES code 1 only					
14. ABSTRACT					
15. SUBJECT TERMS					
16. SECURITY CLASSIFICATION OF:			17. LIMITATION OF ABSTRACT Same as Report (SAR)	18. NUMBER OF PAGES 5	19a. NAME OF RESPONSIBLE PERSON
a. REPORT unclassified	b. ABSTRACT unclassified	c. THIS PAGE unclassified			

density. We introduce the Boussinesq parameter $\beta = LN_0^2/g$ with g the gravitational acceleration. The reduced density ρ is introduced such that $\beta \rho \rho$ is the density perturbation from its background stratification given by ρ_0 . Similarly a reduced pressure is introduced such that ρp is the pressure perturbation. The F term captures external forces such as Coriolis forces and

$$v = \frac{\mu}{\bar{\rho}_0 L^2 N_0}$$

is the Reynolds number. In the Boussinesq approximation ($\beta = 0$) we set $\beta = 0$ in inertial terms but keep a finite β in the buoyancy related terms (those exhibiting the product $N^2 \beta$).

Numerical treatment

Domain discretization. The domain of interest is simulated on logically Cartesian grids in computational space. These can be transformed into moderately complicated representations of real topography by employing grid mappings.

Operator splitting approach. The equations of motion are advanced in time by successively considering the various types of terms that appear. The hyperbolic terms resulting from advection

$$\begin{aligned}\rho_t + (\vec{u} \cdot \nabla) \rho &= 0 \\ \vec{u}_t + (\vec{u} \cdot \nabla) \vec{u} &= \frac{v}{\rho} \nabla^2 \vec{u}\end{aligned}$$

are updated first using an explicit method and with the pressure gradient approximated from the previous time step. Here it is assumed that the time step is not limited by instability of the viscous term. In this step, the quantities that are advanced in time are defined on the cell centers, whereas the advective field is defined on the cell edges.

Then the effect of source terms (gravitational acceleration and terms arising from the coordinate transformation) are added to the velocities defined on the edges of the computational cells, as well as a suitable interpolations of the fluxes calculated for the cell centered velocities

$$\vec{u}_t = -(\rho - \beta N^2 p) \vec{j} + \vec{F}.$$

Finally we perform a projection onto the space of divergence-free velocity fields to enforce the constraint

$$\nabla \cdot \vec{u} = 0$$

on the edge velocities. The potential field is then applied to the cell centered velocities as well to synchronize the two discretized versions of the same field. This operator splitting is carried out at each stage of a low-dissipation Runge-Kutta time stepping procedure.

Grid adaptivity. In adaptive mesh refinement one must identify regions requiring additional resolution by evaluating the local truncation error. Typically this is done through a trial step. This becomes expensive for the full equations of motion due to the effort involved in solving the Poisson equation arising from enforcing the divergence-free constraint. To avoid this, we assume that the hyperbolic terms alone give a sufficiently accurate indication of regions requiring additional resolution and let the grid adaptivity be driven by trial steps of this stage of the operator splitting.

Poisson and Helmholtz solvers.

Each subgrid inherits the boundary conditions for the projection scheme from the edge velocities of the parent grid already projected, so that mass conservation is always enforced. To setup and solve the necessary elliptic solvers, we have developed a package that breaks down the problem in a series of steps: The linear operators corresponding to gradient and divergence (in curvilinear coordinates) are created as a set of sparse matrices in an appropriate representation; next, the numerical laplacian is created as the matrix product of the divergence and gradient operators, ensuring consistency; finally, the resulting linear problem $Ax=b$ is solved using existing highly efficient sparse matrix solvers. The approach is object oriented, and the resulting standalone package (ELLIKIT) can be used to deal with similar problems whenever the field to project is defined on cell edges. In particular, we have implemented hydrostatic and weakly nonhydrostatic approximations that are completely transparent to the end user.

WORK COMPLETED

The main trust this year was devoted to implement the elliptic and parabolic solvers in the self-consistent way described above, in generalized coordinates. We also considered the generation problem of internal waves along the NJ shelf. The SW06 experiments show that arrival time at a given location across-shelf of NLIWs is not well predicted by the baroclinic tidal phase (unlike, e.g., the South China Sea case). Furthermore the largest NLIWs appear to originate during neap-tide. In fact, the barotropic tidal flow is too weak to be able to create directly NLIWs by the standard mechanism of flow over topography. In order to investigate other possible effects, we have considered what effect the presence of a shelf-break front has on the generation process. It is well known that a shelf-break front is present in the area year-around. We have thus conducted a series of experiments in which different combinations of shelf-break strength and stratification are considered.

RESULTS

Model: Figure 1 shows the effect of the shelf break front on the development of the internal tide as the barotropic tide flows over the shelf edge. Here we show the density field at the end of the ebb phase. On the left, the presence of the front causes a much stronger baroclinic response near the shelf edge relative to the control case without front (right). In both cases, the barotropic tide is subcritical.

PUBLICATIONS

A. Scotti, R. Beardsley and B. Butman, “Generation and propagation of nonlinear internal waves in Massachusetts Bay”, in press (2007).

A. Scotti, J. Wendelbo and S. Mitran, “A note on the parameterization of NLIWs in ocean models”, to be submitted to Ocean Modeling (2007).

Software

The implementation of the above method are to be made publicly available to the wider research community in accordance with the grant objectives. Snapshots are periodically made available in the `/applications/2d/Boussinesq` and `/applications/3d/Boussinesq` directories of the

BEARCLAW package (<http://www.amath.unc.edu/Faculty/mitran/bearclaw.html>). ELLIKIT is available at <ftp://ftp.unc.edu/pub/marine/ascotti>

FURTHER WORK

On the modeling side, we are currently exploring how to parameterize NLIWs within hydrostatic models such as ROMS. We are also systematically exploring the effects of the shelf-break front on the generation of NLIWs during SW06.

FIGURES

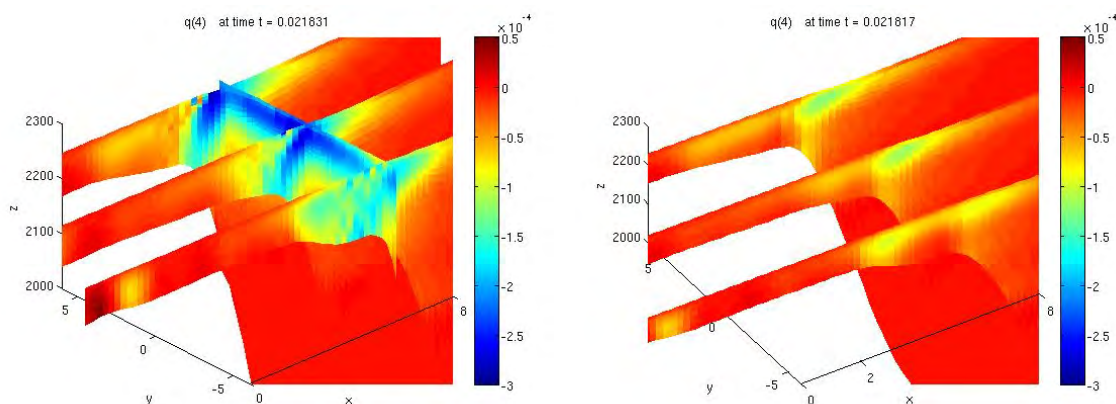


Figure:1 [The figure shows slices of the density field near the shelf edge. One plot shows the field when the shelf-break front is present, the other without a shelfbreak front. In the former case, the baroclinic response is much stronger.]